Psychoneuroendocrinology 106 (2019) 65–76

Contents lists available at ScienceDirect

Psychoneuroendocrinology

journal homepage: www.elsevier.com/locate/psyneuen

Differential effects of TSPO ligands on mitochondrial function in mouse microglia cells

Stefanie Bader[a], Luisa Wolf[a], Vladimir M. Milenkovic[a], Michael Gruber[b], Caroline Nothdurfter[a], Rainer Rupprecht[a], Christian H. Wetzel[a,*]

[a] Department of Psychiatry and Psychotherapy, University of Regensburg, 93953 Regensburg, Germany
[b] Department of Anesthesiology, University of Regensburg, 93953 Regensburg, Germany

ARTICLE INFO

Keywords:
Translocator protein
Mitochondria
Steroid synthesis
Pregnenolone
Mitochondrial membrane potential
Mitochondrial respiration
Cytosolic Ca^{2+} level
Proliferation
Lentiviral knockdown

ABSTRACT

The translocator protein 18 kDa (TSPO), initially characterized as peripheral benzodiazepine receptor, is a conserved outer mitochondrial membrane protein, implicated in cholesterol transport thereby affecting steroid hormone biosynthesis, as well as in general mitochondrial function related to bioenergetics, oxidative stress, and Ca^{2+} homeostasis. TSPO is highly expressed in steroidogenic tissues such as adrenal glands, but shows low expression in the central nervous system. During various disease states such as inflammation, neurodegeneration or cancer, the expression of mitochondrial TSPO in affected tissues is upregulated. The expression of TSPO can be traced for diagnostic purpose by high affinity radio-ligands. Moreover, the function of TSPO is modulated by synthetic as well as endogenous ligands with agonistic or antagonistic properties. Thus, TSPO ligands serve functions as both important biomarkers and putative therapeutic agents.

In the present study, we aimed to characterize the effects of TSPO ligands on mouse BV-2 microglia cells, which express significant levels of TSPO, and analyzed the effect of XBD173, PK11195, and Ro5-4864, as well as the inflammatory reagent Lipopolysaccharides (LPS) on neurosteroid synthesis and on basic mitochondrial functions such as oxidative phosphorylation, mitochondrial membrane potential and Ca^{2+} homeostasis. Specific TSPO-dependent effects were separated from off-target effects by comparing lentiviral TSPO knockdown with shRNA scramble-controls and wild-type BV-2 cells. Our data demonstrate ligand-specific effects on different cellular functions in a TSPO-dependent or independent manner, providing evidence for both specific TSPO-mediated, as well as off-target effects.

1. Introduction

The translocator protein 18 kDa (TSPO) is a conserved multifunctional outer mitochondrial membrane protein (Papadopoulos et al., 2006), which is expressed to varying degrees in multiple tissues. The highest levels of expression are found in steroidogenic cells, while overall expression in the central nervous system is rather low. In the brain, TSPO can be detected predominantly in microglia and reactive astrocytes (Cosenza-Nashat et al., 2009). During diseased states, such as Morbus Alzheimer, Morbus Parkinson, multiple sclerosis, amyotrophic lateral sclerosis, or cancer, TSPO expression in affected tissues is markedly enhanced, suggesting a role for TSPO in the pathophysiology of inflammation and neurodegeneration, as well as in tumor biology. Thus, TSPO is considered as both a diagnostic biomarker, as well as a therapeutic target for treating inflammatory, neoplastic und neurodegenerative diseases (Rupprecht et al., 2010).

Localized to the outer mitochondrial membrane (OMM), TSPO interacts, among others, with the voltage-dependent anion channel (VDAC) and the adenine nucleotide transporter (ANT) (Gatliff et al., 2014; McEnery et al., 1992), supporting its role as a multifunctional protein. TSPO function has been shown to implicate cholesterol transport and affect the synthesis of neurosteroids in neuronal cells (Owen et al., 2017; Papadopoulos et al., 2017; Wolf et al., 2015), steroid synthesis in general (Owen et al., 2017; Papadopoulos et al., 2015), mitochondrial bioenergetics (oxidative phosphorylation, OXPHOS) and metabolism (Liu et al., 2017), beta-oxidation of fatty acids (Tu et al., 2016), production of reactive oxygen species (ROS) (Gatliff et al., 2014), and Ca^{2+} homeostasis (Gatliff et al., 2017). Moreover, TSPO is implicated in cellular downstream processes such as proliferation, survival and apoptosis (Papadopoulos and Lecanu, 2009; Rupprecht et al., 2010).

Initially, the protein was named for its ability to translocate

* Corresponding author.
E-mail address: christian.wetzel@ukr.de (C.H. Wetzel).

https://doi.org/10.1016/j.psyneuen.2019.03.029
Received 12 September 2018; Received in revised form 7 November 2018; Accepted 27 March 2019

cholesterol into the mitochondrial matrix, although this role was questioned in view of various genetic TSPO deletion models (Banati et al., 2014; Morohaku et al., 2014; Papadopoulos et al., 2017; Tu et al., 2014). Thus, the accurate function of TSPO in physiology and pathophysiology is still under intensive investigation. The TSPO protein possesses high affinity binding sites for endogenous ligands, such as cholesterol, heme/protoporphyrin, acyl-CoA-binding peptide, and the diazepam-binding inhibitor peptide (Papadopoulos and Lecanu, 2009). Moreover, an increasing number of synthetic compounds is generated to target a high affinity binding site at the TSPO protein and function as diagnostic or therapeutic drugs, such as cholesterol-, indole- and benzodiazepine-derivatives (Kim and Pae, 2016a,b). However, in face of the multifunctional nature of TSPO and the different pharmacological properties of the various TSPO ligands, there is still need for deeper understanding of the functions and mechanisms of action initiated by the individual compounds.

To shed light on the functional profile, as well as agonistic or antagonistic properties of TSPO ligands, we used mouse BV-2 microglia cells, which are known to express TSPO and possess steroidogenic capacity (Wolf et al., 2015). We investigated the effect of the established TSPO ligands XBD173, PK11195, Ro5-4864, and the inflammatory reagent LPS on steroid synthesis, as well as on basic mitochondrial functions and properties such as OXPHOS, the mitochondrial membrane potential (MMP), and Ca^{2+} homeostasis. To separate specific TSPO-dependent action from off-target effects, we compared lentiviral TSPO knockdown cells with shRNA scramble-controls and wild-type BV-2 cells.

2. Results

2.1. Regulation of TSPO protein expression in BV-2 microglia cells

In order to investigate the direct effect of TSPO ligands on mitochondrial protein expression in microglial cells, we incubated wild-type BV-2 cells with XBD173 (10 μM), PK11195 (100 nM), or Ro5-4864 (100 nM) and analyzed TSPO protein expression after 24 h. As an alternative to directly acting TSPO ligands, we incubated the cells with the prototypical endotoxin LPS (100 ng/ml) to activate the microglial cell line and to induce an inflammatory response (Chen et al., 2012). The concentration of compounds in the experiments were adjusted according to the respective maximal sublethal toxic concentration as demonstrated by the WST-1 viability assay using a range from 1 nM to 100 μM (data not shown). Our data show that XBD173, PK11195, and Ro5-4864 caused a slight increase in mean TSPO protein expression (to 133–151% of wild-type control, n = 7) which did not reach significance, whereas the treatment of the cells with LPS induced a significant increase in TSPO protein expression to on average 147 ± 14.9% (n = 7, p = 0.008, t-test) (Fig. 1).

Consequently, cellular inflammation, as induced by treating mouse microglia cells with LPS, lead to a significant increase in TSPO protein expression. Our findings are in line with the observation that elevated levels of TSPO expression could serve as a marker for inflammatory processes in the central and peripheral neural system of rodents.

2.2. TSPO knockdown by lentiviral expression of TSPO-shRNA

To investigate the specific function of TSPO ligands in BV-2 mouse microglia cells, we performed a lentiviral TSPO knockdown, which led to strongly reduced TSPO protein levels in transduced cells. This allowed us to compare the impact of TSPO ligands on various mitochondrial and cellular functions in cells that express either physiological (scramble shRNA-treated), or strongly reduced levels of mitochondrial TSPO, respectively, thereby separating TSPO-dependent from off-target effects.

Transduction of BV-2 cells with lentivirus coding for TSPO-shRNA led to a marked reduction in TSPO protein expression compared to scr-

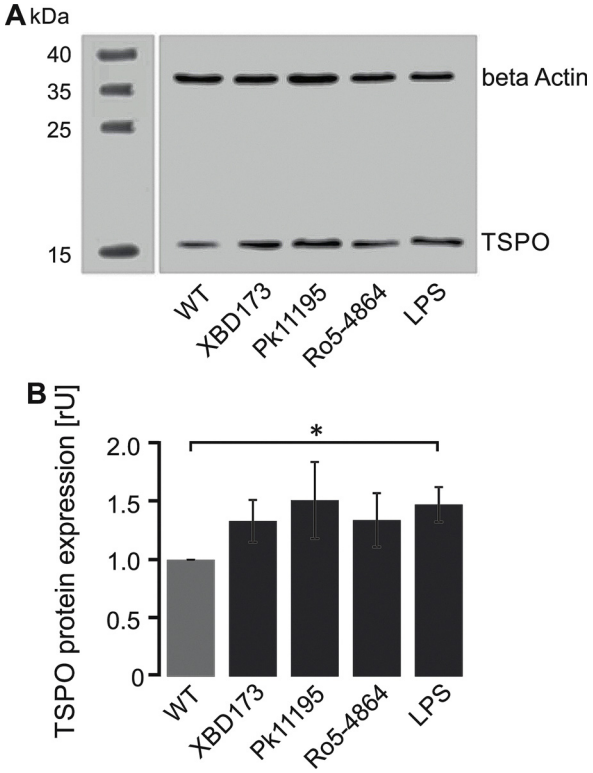

Fig. 1. Impact of TSPO ligands or LPS on the expression of mitochondrial TSPO protein in mouse BV-2 cells. (A) Western blot shows relative expression of TSPO protein in BV-2 cells treated with the TSPO ligands XBD173 (10 μM), PK11195 (100 nM), Ro5-4864 (100 nM) or with inflammatory LPS (100 ng/ml). (B) Diagram shows densitometric analysis of TSPO expression. Values are normalized to the expression level of beta-actin.

shRNA-treated or untreated wild-type BV-2 cells. Normalized TSPO protein level is reduced by about 84% within 10 days after lentiviral TSPO-shRNA-treatment, whereas scr-shRNA did not alter TSPO protein expression (n = 6) (Fig. 2A–B).

In addition, analysis of mRNA expression by Real-Time qPCR revealed a significant reduction of TSPO mRNA in TSPO knock-down cells compared with scr-shRNA-treated BV-2 cells. Scramble BV-2 cells expressed 48 times more TSPO mRNA than TSPO knockdown cells (Fig. 2C). Moreover, Ct values of Cyp11A1 (*P450scc*) suggested a prominent expression of Cyp11A1 mRNA, which was not influenced by knocking down TSPO expression. The expression of the steroidogenic acute regulatory protein (StAR) mRNA was rather low and did not change upon knock-down of TSPO mRNA (Supplemental Fig. S1).Reduced TSPO protein expression after lentiviral TSPO-shRNA infection is also demonstrated in the decreased immunofluorescence shown in Fig. 2D. Mitochondrial fluorescence resulting from anti-ATP synthase immunostaining does not appear to be different between TSPO knockdown or scr cells, suggesting that mitochondrial gross morphology in BV-2 cells is not affected by TSPO knockdown.

2.3. The TSPO ligand XBD173 specifically affects steroid biosynthesis in BV-2 microglial cells

TSPO has been reported to play an essential role in mitochondrial cholesterol transport making it a key regulator of steroid synthesis. We aimed to investigate the impact of TSPO ligands on the biosynthesis of neurosteroids in mouse microglial cells. Following the hypothesis that TSPO mediates an essential step in neurosteroid synthesis, we analyzed the levels of pregnenolone, which is the first steroid produced from cholesterol, probably by the activity of cytochrome P450scc in the mitochondrial matrix. The assay was performed in the presence of

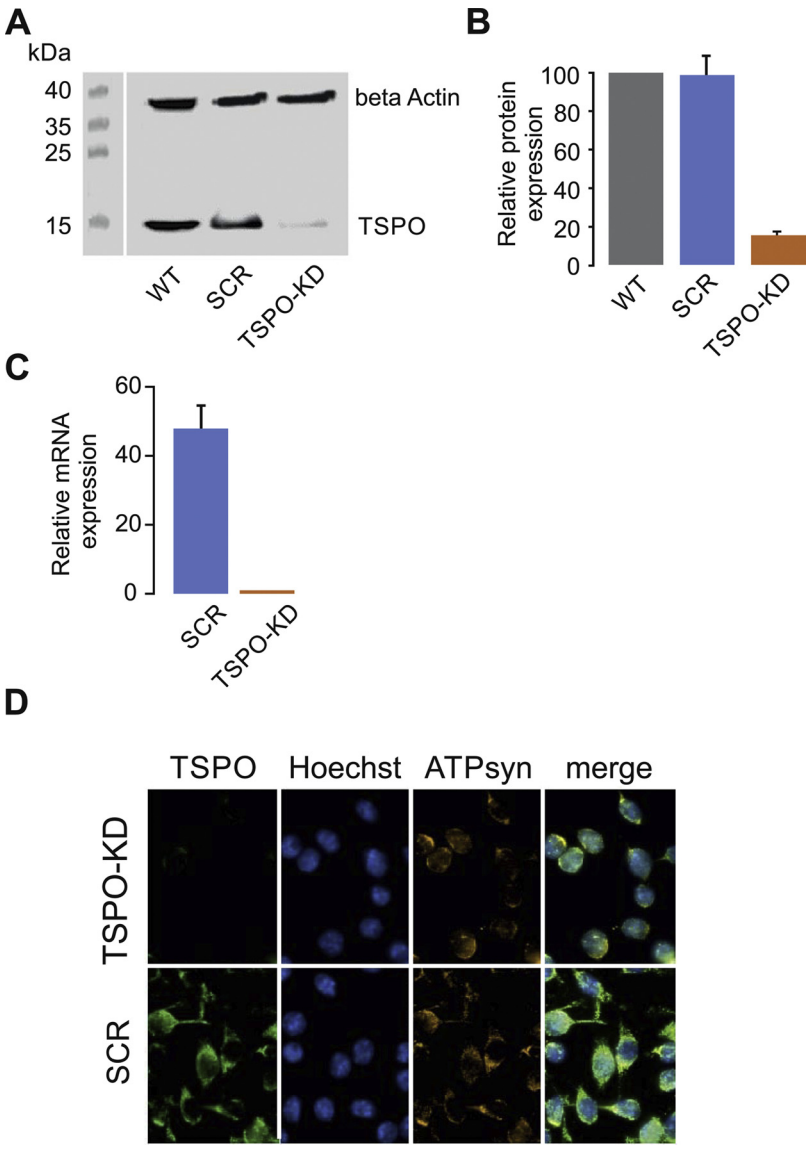

Fig. 2. Lentiviral TSPO-shRNA expression led to knockdown of TSPO protein in BV-2 cells. (A) Western blot demonstrates the reduced expression of TSPO protein 10 days after lentiviral infection of BV-2 cells. (B) Expression level is normalized to the expression of beta-actin. (C) Analysis of mRNA expression by Real-Time qPCR revealed a significantly lower abundance of TSPO mRNA in TSPO knock-down cells compared with scr-shRNA-treated BV-2 cells. Ct values of Cyp11A1 (*P450scc*) suggested a prominent expression of Cyp11 A1 mRNA, which was not influenced by knocking down TSPO expression. The expression of the steroidogenic acute regulatory protein (StAR) mRNA was rather low and did not change upon knock-down of TSPO mRNA. (D) Immunofluorescence shows reduced labelling of TSPO in knock-down cells compared with BV-2 cells infected with scr-shRNA expressing lentivirus. Fluorescence of mitochondria as probed with anti-ATP synthase antibody is not different between TSPO knockdown and scramble controls.

trilostane (25 μM, 8 h) to prevent further metabolism of newly synthesized pregnenolone by inhibiting the enzyme 3β-hydroxysteroid dehydrogenase. Performing a pregnenolone ELISA, we found that supernatants collected from TSPO knockdown cells contained a significantly lower concentration of pregnenolone than from scramble-shRNA-treated control cells (4.8 ± 0.2 ng/ml vs. 7.8 ± 0.4 ng/ml, n = 4, p = 0.0003, t-test). Moreover, challenging the cells with the TSPO ligand XBD173 (10 μM, 24 h) significantly stimulated pregnenolone synthesis in TSPO expressing scr-shRNA-treated cells (14.3 ± 0.8 ng/ml, n = 4, p = 0.00003, t-test), but has no stimulatory effect on pregnenolone synthesis in TSPO knockdown cells (5.1 ± 0.2 ng/ml, n = 4) (Fig. 3A). In contrast to the stimulatory effect of XBD173, the TSPO ligands PK11195 (100 nM) and Ro5-4864 (100 nM) as well as LPS treatment (100 ng/ml) did not enhance the synthesis of pregnenolone in scramble-shRNA control BV-2 cells. Our observation that the concentration of pregnenolone in the supernatant of cultivated TSPO knockdown cells was significantly lower than in that of scr-shRNA control cells, indicates that BV-2 cells possess a basic pregnenolone synthesizing capacity which was dependent on the expression of TSPO. This basic pregnenolone concentration was reduced by pharmacological treatment with the supposed TSPO antagonist PK11195, but also with the agonistic Ro5-4864 or LPS, and reached levels as low as with lentiviral knockdown of TSPO (Fig. 3A).

These results were confirmed in a second set of experiments by means of gas chromatography-mass spectrometry (GC–MS). The basal level of pregnenolone was lower in supernatants of TSPO knockdown BV-2 cells (5.3 ± 1.2 ng/ml) than in scr controls (10.6 ± 1.3 ng/ml) (n = 4), again supporting the hypothesis that TSPO modulates pregnenolone synthesis. Treating the BV-2 scr-shRNA control cells with XBD173 (10 μM) significantly increased pregnenolone levels (19.5 ± 3.4 ng/ml; n = 4, p = 0.048, t-test), whereas PK11195 (100 nM), Ro5-4864 (100 nM), and LPS-treatment (100 ng/ml) did not stimulate the synthesis of pregnenolone (Fig. 3B).

These findings demonstrate that XBD173 stimulates pregnenolone synthesis in BV-2 cells in a TSPO-dependent manner. However, with regard to neurosteroid synthesis the other compounds tested did not show an agonistic activity at TSPO in our set up. Moreover, our data are in favor of a general role of TSPO in steroid synthesis.

2.4. TSPO ligands affect the mitochondrial membrane potential

To investigate the impact of TSPO ligands on bioenergetics and mitochondrial function in BV-2 cells, we analyzed the effects of XBD173, PK11195, Ro5-4864, and LPS on the mitochondrial membrane potential (MMP) by loading scramble control or TSPO knockdown BV-2 cells with a combination of the cationic dyes TMRE (30 nM, non-

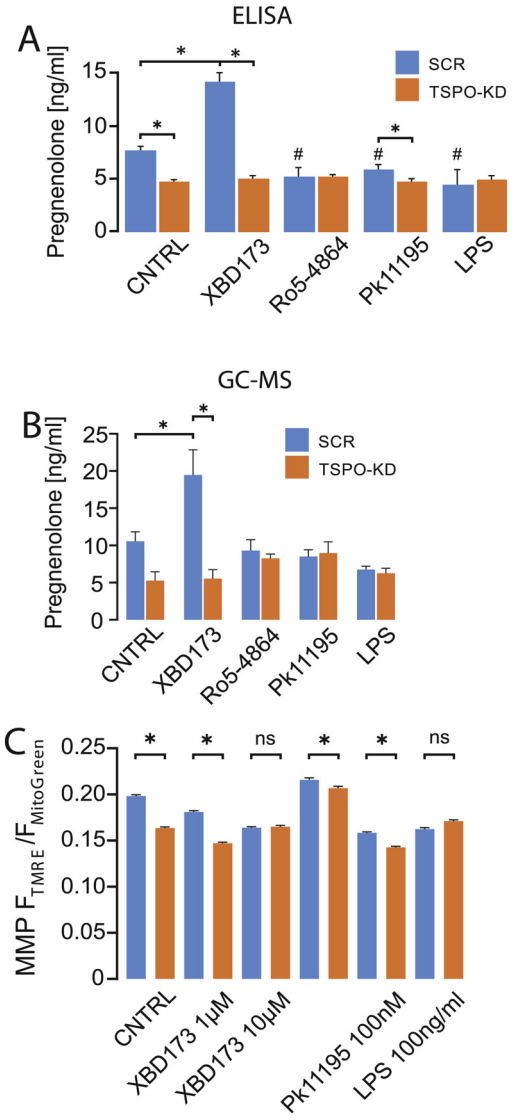

Fig. 3. TSPO ligands stimulate pregnenolone synthesis in BV-2 cells in a TSPO-dependent manner and affect mitochondrial membrane potential. Diagram shows pregnenolone concentration [ng/ml] measured by ELISA (A) or gas chromatography/mass spectrometry (B) in the supernatants of cultivated TSPO knockdown or scramble BV-2 control cells after treatment with TSPO ligands or LPS (24 h), respectively. XBD173 (10 µM), PK11195 (100 nM), Ro5-4864 (100 nM), LPS (100 ng/ml). Trilostane (25 µM) was added 8 h prior to sampling. Pregnenolone concentration is reduced in TSPO knockdown cells. Treatment of scr-shRNA BV-2 cells with XBD173 significantly enhanced pregnenolone synthesis. (C) Diagram shows the effect of TSPO expression and the TSPO ligands XBD173 (1 µM, 10 µM), PK11195 (100 nM), Ro5-4864 (100 nM), as well as treatment with LPS (100 ng/ml), on mitochondrial membrane potential (MMP). The MMP is expressed as a fluorescence ratio given by the intensity of the TMRE fluorescence divided by the intensity of the MitoTracker Green fluorescence in multiple regions of interest. # means significantly different from scramble control. § means significantly different from TSPO-KD control.

quenching mode) and Mitotracker Green (MitoGreen, 1 µM). The extent to which TMRE accumulates in the mitochondrial membranes is dependent on the strength of the applied electric field. For normalization of the TMRE fluorescence, we additionally stained the mitochondria with the mitochondria specific dye MitoTracker Green, which is nearly independent of the membrane potential and we analyzed the ratio of the fluorescence signals emitted by the two dyes. The ratio $F_{TMRE}/F_{MitoGreen}$ is therefore a measure for the strength of the MMP (Chaudhuri et al., 2016).

We found that knocking down TSPO protein in BV-2 cells decreased the fluorescence ratio from 0.20 ± 0.0015 (n = 1252 cells in 5 independent experiments) to 0.16 ± 0.0011 (n = 1224 cells in 5 independent experiments, $p < 0.0001$), indicating that the presence of TSPO significantly affects the MMP (Fig. 3C, Tables 1A and 1B). Treating the BV-2 cells with 1 or 10 µM XBD173, led to a concentration-dependent reduction in MMP in scramble BV-2 cells (0.18 ± 0.0015, n = 807 cells in 3 independent experiments, $p < 0.0001$, and 0.16 ± 0.0014, n = 825 in 3 independent experiments, $p < 0.0001$, respectively). However, in BV-2 TSPO knockdown cells, MMP was affected only by 1 µM XBD173 (0.15 ± 0.0011, n = 940 cells in 3 independent experiments; $p < 0.0001$), whereas 10 µM of this compound did not affect the fluorescence ratio (0.17 ± 0.0014, n = 857 cells in 3 independent experiments; $p > 0.9999$). These data indicate that XBD173 exerts both TSPO-dependent and independent effects on the MMP in BV-2 cells, but to a different extent and depending on the ligand concentration. Ro5-4864 (100 nM) increased the MMP in both BV-2 scramble (0.22 ± 0.0025, n = 1623 in 6 independent experiments, $p < 0.0001$) and TSPO knockdown cells (0.21 ± 0.0023, n = 1735 in 6 independent experiments, $p = 0.0003$). Treating the cells with 100 nM PK11195 reduced the TMRE/MitoGreen fluorescence ratio in scramble and TSPO knockdown cells to a different extent (to 0.16 ± 0.0011, n = 1289 in 5 independent experiments, $p < 0.0001$, and 0.14 ± 0.0013, n = 1233 cells in 5 independent experiments, $p < 0.0001$, respectively), pointing again to a combination of TSPO-dependent and independent effects. The effect of LPS (100 ng/ml) on the MMP seems to be strongly dependent on the expression of TSPO, since this compound did not significantly affect the MMP in knockdown BV-2 cells (0.17 ± 0.0014, n = 844 in 3 independent experiments, n.s. $p = 0.089$), but in scramble BV-2 cells (0.16 ± 0.0016, n = 633 in 3 independent experiments, $p < 0.0001$).

2.5. Effect of TSPO ligands on intracellular Ca^{2+} homeostasis

Driven by their negative membrane potential, mitochondria attract calcium ions and accumulate them in the matrix, thereby contributing to the regulation of intracellular $[Ca^{2+}]$. The extent to which mitochondria accumulate or release calcium ions represents the Ca^{2+} buffering capacity, and has both beneficial and detrimental effects, as it contributes to Ca^{2+} homeostasis, but also triggers apoptosis in response to excitotoxicity-induced Ca^{2+} overload (Giorgi et al., 2012). We investigated the effects of TSPO ligands on Ca^{2+} homeostasis in TSPO knockdown and scr-shRNA-treated BV-2 cells by loading the cells with the ratiometric Ca^{2+} sensitive dye Fura-2/AM. A preceding application of 100 µM ATP induced an increase of intracellular Ca^{2+} by stimulating plasma membrane ionotropic P2X and metabotropic P2Y receptors (Gilbert et al., 2016). The subsequent mitochondrial Ca^{2+} uptake contributes to the removal of cytosolic calcium ions to an extent which is dependent on the MMP as well as on the functional properties of Ca^{2+} conducting channels (e.g. VDAC), and the activity of Ca^{2+} transporting proteins in the inner mitochondrial membrane (e.g. mitochondrial calcium uniporter, MCU). This capacity can be analyzed by treating the cells with the ETC/OXPHOS uncoupling agent FCCP (10–20 µM), which clears the mitochondrial proton gradient, thereby leading to dissipation of the MMP. Consequently, Ca^{2+} is released upon FCCP treatment from the mitochondrial matrix and can be analyzed as a transient increase in cytosolic $[Ca^{2+}]$ (Fig. 4A).

We analyzed the amplitudes of FCCP-induced Ca^{2+} transients and found that the mitochondrial Ca^{2+} release in TSPO knockdown cells (n = 142) was not different from scramble cells (n = 170) under basal conditions ($p = 0.98$). Incubation of the cells with 1 µM XBD173 did not influence the FCCP-induced Ca^{2+} release neither in scr BV-2, nor in TSPO knock-down cells ($p = 0.075$). However, treatment with 10 µM XBD173, PK1119 (100 nM) or LPS (100 ng/ml) reduced the FCCP-induced Ca^{2+} release in scr BV-2 cells (solvent control vs. XBD173,

Table 1A
Statistical test (one-way ANOVA) for the effect of TSPO ligands or LPS on the mitochondrial membrane potential in scramble BV-2 or TSPO knockdown cells. P values indicate the level of significance, n.s. = not significant.

Effect of TSPO ligands and LPS (vs. solvent control) on mitochondrial membrane potential in scramble CNTRL or TSPO knockdown cells					
	XBD173 (1 μM)	XBD173 (10 μM)	Ro5-4864 (100 nM)	PK11195 (100 nM)	LPS (100 ng/ml)
BV-2 scramble	< 0.0001	< 0.0001	< 0.0001	< 0.0001	< 0.0001
TSPO knockdown	< 0.0001	n.s.	< 0.0001	< 0.0001	n.s.

Table 1B
Statistical test (one-way ANOVA) for the effect of TSPO expression on the mitochondrial membrane potential in pharmacologically treated BV-2 cells. P values indicate the level of significance, n.s. = not significant.

Effect of TSPO expression (BV-2 scramble vs. TSPO knockdown) on the mitochondrial membrane potential in pharmacologically treated cells						
	solvent control	XBD173 (1 μM)	XBD173 (10 μM)	Ro5-4864 (100 nM)	PK11195 (100 nM)	LPS (100 ng/ml)
scramble vs. knockdown	< 0.0001	< 0.0001	n.s.	0.0003	< 0.0001	n.s.

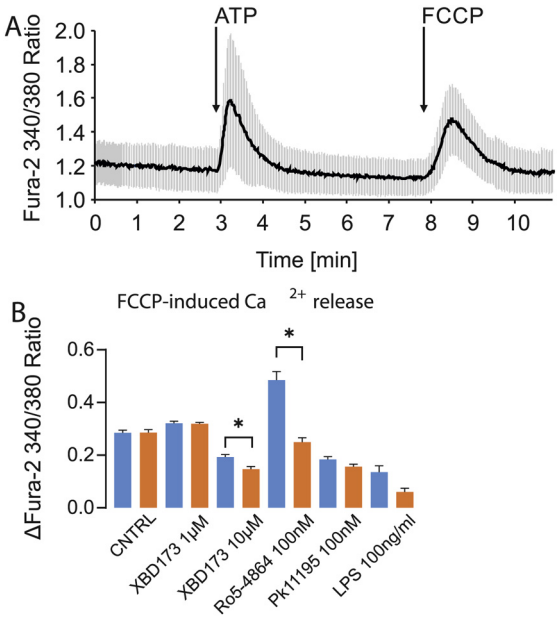

Fig. 4. Impact of TSPO ligands on Ca^{2+} homeostasis. (A) Transient increase of intracellular [Ca^{2+}] in BV-2 cells mediated by plasma membrane P2X purine and ER IP3 receptors as well as by mitochondrial release. Imaging of Fura-2/AM loaded BV-2 cells indicates intracellular [Ca^{2+}]. The application of ATP (100 μM) stimulated both ionotropic and metabotropic purine receptors. The uncoupling compound FCCP (10–20 μM) led to dissipation of the mitochondrial membrane potential and released Ca^{2+} from the mitochondria by removing the Ca^{2+}-accumulating/retaining force. (B) Impact of TSPO ligands on Ca^{2+} homeostasis. Diagram shows FCCP-induced changes in Fura-2 fluorescence ($\Delta F_{340}/F_{380}$) in Fura-2/AM-loaded BV-2 cells. The FCCP-induced release of mitochondrial Ca^{2+} is increased by Ro5-4864 by a TSPO-dependent mechanism. # means significantly different from scramble control. # means significantly different from scramble control. § means significantly different from TSPO-KD control.

n = 146, p < 0.001; solvent control vs. PK11195, n = 170, p < 0.001; solvent control vs. LPS, n = 26, p < 0.001), with a more pronounced effect on TSPO knockdown BV-2 cells (n = 118, p < 0.001; n = 143, p < 0.001; n = 13, p < 0.001, respectively). Interestingly, Ro5-4864 (100 nM) markedly increased the FCCP-induced Ca^{2+} signal in scr BV-2 control cells (n = 59, p < 001), but has no effect on TSPO knockdown cells (n = 75, p = 0.08), pointing to a specific and TSPO-dependent effect of Ro5-4864 on Ca^{2+} homeostasis in BV-2 cells (Fig. 4B).

2.6. Impact of TSPO ligands on mitochondrial respiration

The effect of TSPO ligands on mitochondrial respiration in BV-2 cells was studied by analyzing the oxygen consumption rate (OCR) using the Seahorse Flux Analyzer (Agilent Technologies) in non-permeabilized TSPO knockdown and scr-shRNA treated control cells (Fig. 5). Focusing on the effect of TSPO expression, we found a significantly increased non-mitochondrial respiration, proton leak, and a decreased spare capacity, and coupling efficiency in pharmacologically untreated (solvent control, CNTRL) TSPO knockdown cells compared to scramble controls (Table 2). This finding is in line with experiments demonstrating that the TSPO expression level affects mitochondrial energetics (Tu et al., 2016).

Treating the cells with XBD173 (1 μM or 10 μM) did not differentially affect respiration of TSPO knock-down vs. scramble BV-2 cells. Ro5-4864 (100 nM) affected the maximal respiration and proton leak, as well as the coupling efficiency, whereas PK11195 (100 nM) affected only the coupling efficiency in TSPO knock-down vs. scramble control cells.

Focusing on the effect of pharmacological treatment, we found a significant effect of Ro5-4864 and PK11195 on the basal and ATP-related respiration as well as XBD173, Ro5-4864 and PK11195 on the spare capacity in scramble BV-2, but not TSPO knock-down cells, indicating a TSPO-specific effect of these ligands on the respective respiratory parameters (Table 3 and Fig. 5). However, in TSPO knockdown cells, XBD173 altered the non-mitochondrial respiration and XBD173, Ro5-4864, and PK11195 had a significant effect on the coupling efficiency, which was not observed in the scramble control cells (Table 3 and Fig. 5).

2.7. Impact of TSPO ligands on proliferation of BV-2 cells

The effect of TSPO ligands on the proliferation kinetics of BV-2 cells was investigated by performing a cell growth assay. We analyzed the change in confluency over time as a measure of cell proliferation and compared TSPO knockdown with scramble BV-2 cells in the presence of solvent control (ethanol), XBD173 (10 μM), PK11195 (100 nM), Ro5-4864 (100 nM), or LPS (100 ng/ml), respectively. We found a reduced proliferation in untreated TSPO knockdown cells (corresponding with a

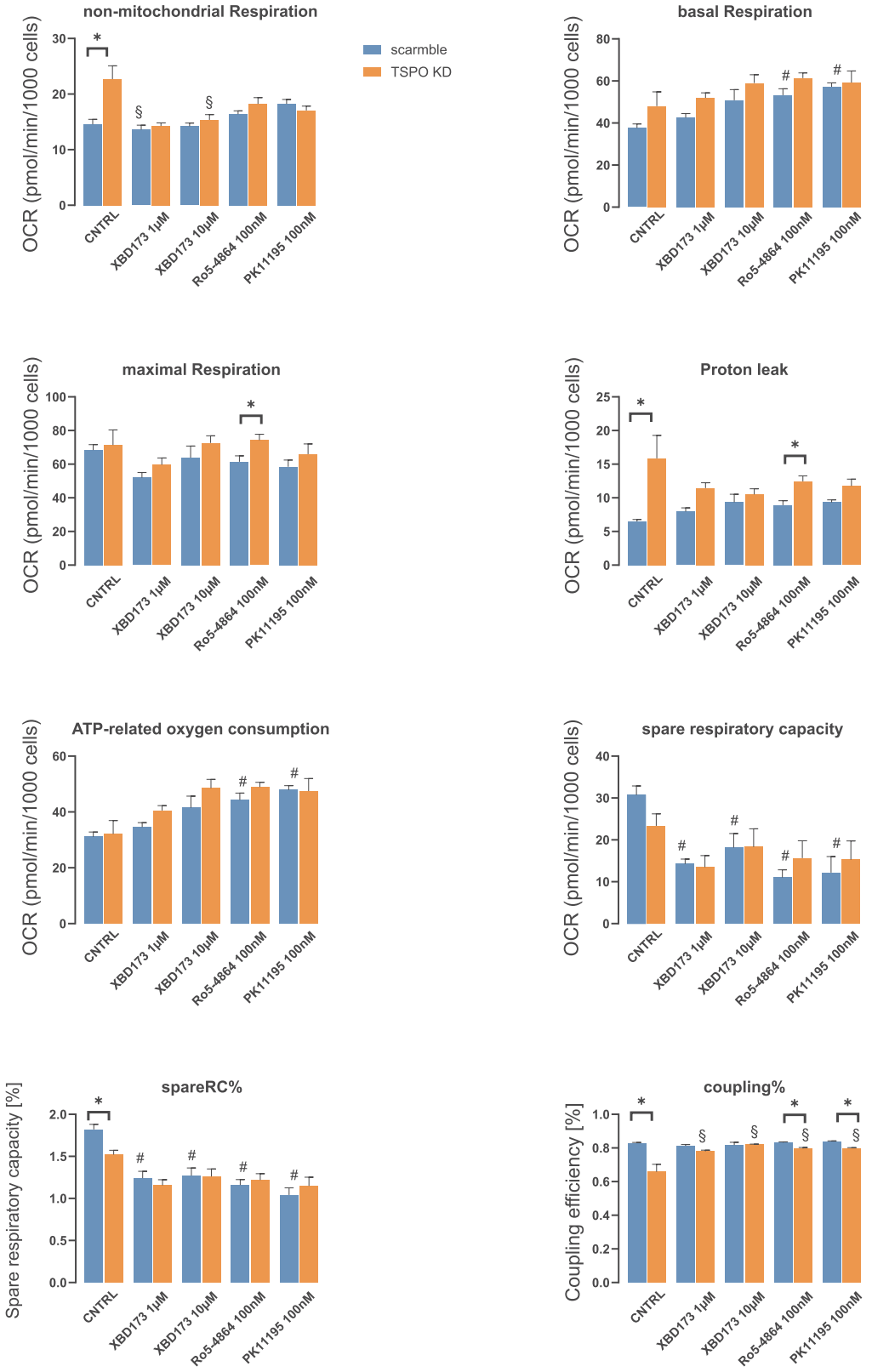

Fig. 5. Impact of TSPO expression and TSPO ligands on the oxygen consumption rate. Oxidative phosphorylation is analyzed by assessing the oxygen consumption rate (OCR) in non-permeabilized BV-2 scramble and TSPO knockdown cells. Data show OCR of non-mitochondrial oxygen consumption, proton leak, basal and maximal respiration, ATP-related oxygen consumption, and spare respiratory capacity as well as coupling efficiency (mean ± SE). See the text for details. # means significantly different from scramble control. § means significantly different from TSPO-KD control.

Table 2
Statistical test for the effect of BV-2 genotype (TSPO knockdown vs. scramble) on the oxygen consumption rate at the indicated experimental conditions. P values indicate the level of significance, n.s. = not significant.

Effect of BV-2 genotype (scramble vs. TSPO knockdown) on oxygen consumption					
	CNTRL	XBD173 (1 μM)	XBD173 (10 μM)	Ro5-4864 (100 nM)	PK11195 (100 nM)
Non-mitochondrial respiration	0.005	n.s.	n.s.	n.s.	n.s.
Basal respiration	n.s.	n.s. (0.053)	n.s.	n.s.	n.s.
Maximal respiration	n.s.	n.s.	n.s.	0.044	n.s.
Proton leak	0.015	n.s. (0.059)	n.s.	0.030	n.s.
ATP-related respiration	n.s.	n.s. (0.057)	n.s.	n.s.	n.s.
Spare capacity [%]	0.002	n.s.	n.s.	n.s.	n.s.
Coupling efficiency [%]	0.002	n.s.	n.s.	0.005	0.000

reduced time constant from b = 0.037 ± 0.001 to b = 0.031 ± 0.001; n = 6; p = 0.0243, 2way ANOVA, multiple comparison), indicating that the expression level of TSPO has an influence on the proliferation rate of BV-2 cells. In addition, the time constant of proliferation in scramble BV-2 cells was significantly changed by treating the cells with LPS (100 ng/ml) (n = 6; p = 0.0108, 2way ANOVA, multiple comparison) (Fig. 6), favoring the hypothesis that the effect of LPS on proliferation is mediated by TSPO.

3. Discussion

The translocator Protein 18 kDa (TSPO) resides in the outer mitochondrial membrane where it is supposed to be involved in cholesterol transport and steroid hormone synthesis, in regulation of cellular energy production and Ca^{2+} homeostasis, as well as in the generation of reactive oxygen species (Gatliff et al., 2017; Papadopoulos et al., 2017). Recent TSPO knock-out studies revealed controversial results about how TSPO deletion affects steroidogenesis (Banati et al., 2014; Morohaku et al., 2014; Papadopoulos et al., 2017; Tu et al., 2014). Biosynthesis of steroid hormones is mainly performed by the adrenal glands, gonads, placenta, thymus, skin and the brain (Costa et al., 2018). However, the role of TSPO in the synthesis of neurosteroids in the CNS is still under investigation.

We aimed to shed light on the impact of TSPO ligands on cellular physiology in mouse microglia BV-2 cells. By investigating the effects of TSPO ligands on BV-2 cells with strongly reduced TSPO expression (TSPO knockdown by lentiviral expression of TSPO-shRNA) and comparing the results with appropriate controls (scramble-shRNA), we sought to separate specific TSPO-dependent effects from off-target

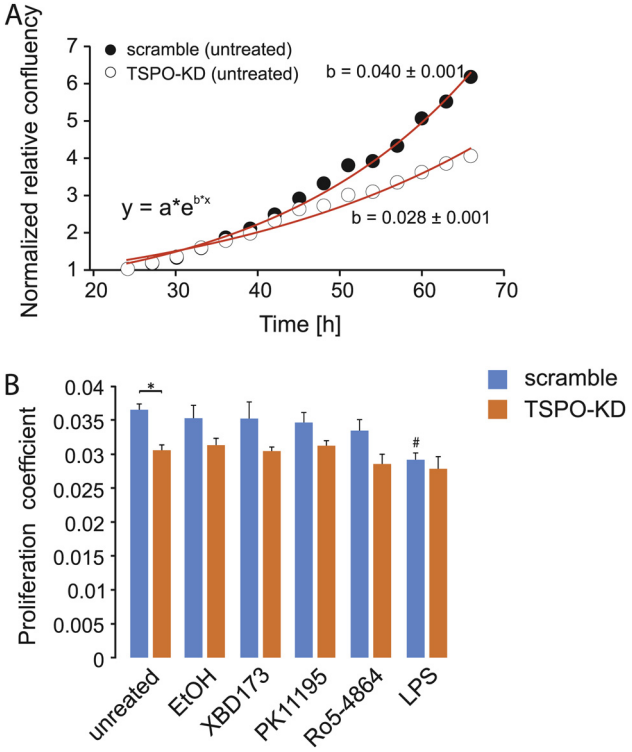

Fig. 6. Impact of TSPO expression and TSPO ligands on proliferation of BV-2 cells. (A) Proliferation of scramble and TSPO knockdown BV-2 cells was assayed analyzing the change in confluency in the culture plate over time. Cells were grown for 24 h before treatment with indicated compounds. (A) Representative proliferation curve showing the change in confluency in untreated BV-2 scramble or TSPO knockdown cells. The data are normalized to the first data point at the time of pharmacological treatment. The proliferation rate is analyzed by approximating the data with an exponential fit ($y = a*e^{b*x}$). The coefficient b is a measure for the rate of proliferation. (B) Diagram shows the proliferation coefficients in BV-2 scramble and TSPO knockdown cells at the indicated treatment. Untreated TSPO knockdown cells showed a slower proliferation (corresponding with a reduced time constant from b = 0.037 ± 0.001 to b = 0.031 ± 0.001; n = 6; p = 0.0243, 2way ANOVA, multiple comparison). The time constant of proliferation in scramble BV-2 cells was significantly changed by treating the cells with LPS (100 ng/ml) (n = 6; p = 0.0108, 2way ANOVA, multiple comparison. # means significantly different from scramble control.

Table 3
Statistical test for the effect of pharmacological treatment (XBD173, PK11195, and Ro5–4864 vs. control) on the oxygen consumption rate at the indicated genotype (scramble or TSPO knockdown). P values indicate the level of significance, n.s. = not significant.

Effect of pharmacological treatment of BV-2 cells on oxygen consumption rate								
	Scramble				TSPO knockdown			
	XBD173 (1 μM)	XBD173 (10 μM)	Ro5-4864 (100 nM)	PK11195 (100 nM)	XBD173 (1 μM	XBD173 (10 μM)	Ro5-4864 (100 nM)	PK11195 (100 nM)
Non-mitochondrial respiration	n.s.	n.s.	n.s.	n.s.	0.005	0.008	n.s.	n.s.
Basal respiration	n.s.	n.s.	0.04	0.007	n.s.	n.s.	n.s.	n.s.
Maximal respiration	n.s.	n.s.	n.s.	n.s.	n.s.	n.s.	n.s.	n.s.
Proton leak	n.s.	n.s.	n.s.	n.s.	n.s.	n.s.	n.s.	n.s.
ATP-related respiration	n.s.	n.s.	0.033	0.004	n.s.	n.s.	n.s.	n.s.
Spare capacity	0.000	0.000	0.000	0.000	n.s.	n.s.	n.s.	n.s.
Spare capacity [%]	0.001	0.013	0.000	0.000	n.s.	n.s.	n.s.	n.s.
Coupling efficiency [%]	n.s.	n.s.	n.s.	n.s.	0.010	0.000	0.008	0.002

effects of TSPO ligands, which do not involve TSPO function (Sileikyte et al., 2014; Tu et al., 2015).

3.1. Effect of TSPO ligands on steroid synthesis

We found that the basal pregnenolone concentration was significantly reduced in TSPO knockdown compared with scramble control cells. Moreover, treatment with XBD173 (10 μM) increased pregnenolone concentration only in control cells, while TSPO knockdown cells were not affected. In contrast to XBD173, the high affinity TSPO ligands PK11195 (100 nM) and Ro5-4864 (100 nM), as well as the inflammatory agent LPS (100 ng/ml) had no effect on pregnenolone concentration, neither in scramble nor in TSPO knockdown cells. Our data indicate that TSPO is specifically involved in neurosteroid synthesis in mouse microglial BV-2 cells, and that the presence of TSPO is mandatory for the stimulatory effect of XBD173. Moreover, the observation that the high affinity ligands PK11195 and Ro5-4864 did not affect neurosteroid synthesis in our model, points to a more differentiated spectrum of TSPO ligand/receptor interactions with agonistic or antagonistic properties. Analysis of the thermodynamic properties suggested an agonistic or antagonistic behavior of various ligands (Le Fur et al., 1983), although such pharmacological assignment was found to be not always applicable in in vivo and in vitro studies (Choi et al., 2011; Papadopoulos and Lecanu, 2009). A differing pharmacological profile is also supported by the earlier observation that PK11195 is able to inhibit the neurosteroid-inducing effects of other TSPO binding drugs such as FGIN-1-27 (Korneyev et al., 1993), indoleacetamides (Kozikowski et al., 1993), YL-IPA08 (Zhang et al., 2014), and diazepam-binding inhibitor TTN (Do-Rego et al., 1998). Moreover, Tu et al. (2015) reported that the effect of PK11195 on steroidogenesis in MA-10 mouse Leydig tumor cells is not mediated by TSPO (Tu et al., 2015). However, the authors of this study used a hundred times higher concentration of PK11195 (10 μM). Given the high lipophilicity of PK11195, this elevated concentration may trigger additional effects that can occur even in the absence of TSPO.

Additionally, Ro5-4864 was reported to act as a convulsing (Weissman et al., 1983) and anxiogenic substance (File and Lister, 1983), but was also discussed as being a TSPO agonist (Le Fur et al., 1983; Selvaraj and Tu, 2016), which possesses neuroprotective properties (Palzur et al., 2016). Costa and co-workers reported a stimulatory effect of PK11195 and Ro5-4864 on pregnenolone synthesis in rat C6 glioma and human U87MG cells (Costa et al., 2016b; Da Pozzo et al., 2016), however, with a markedly lower potency compared with XBD173 (Costa et al., 2016a).

3.2. Effect of TSPO ligands on Ca^{2+} homeostasis and mitochondrial membrane potential

Mainly driven by their negative membrane potential, mitochondria contribute to the intracellular Ca^{2+} homeostasis. It has already been shown in the 1960s that isolated mitochondria are able to accumulate Ca^{2+} (Vasington and Murphy, 1962). We found that TSPO knockdown in BV-2 cells did not alter Ca^{2+} storing capacity, as indicated by the unchanged FCCP-induced Ca^{2+} release. However, we did find a change in the MMP of TSPO-knock down cells when compared to scramble controls. Distinct from our knockdown approach, Gatliff et al. (2017) reported a deregulation of mitochondrial Ca^{2+} concentration by overexpression of TSPO in MEFs, HeLa, and CF35 cells. The effects they observed in mitochondrial Ca^{2+} handling were found to be consistent with the changes which they found in mitochondrial membrane potential (Gatliff et al., 2017). Our observation that the effect of TSPO ligands on FCCP-induced Ca^{2+} release and mitochondrial membrane potential did not directly correlate, indicate that these two functional parameters might be regulated separately to a certain extent, and that TSPO ligands may also interfere with mechanisms which are in part independent from TSPO to modulate mitochondrial membrane potential and Ca^{2+} homeostasis.

A differential effect of TSPO ligands on Ca^{2+} homeostasis is also reported in the literature. In mitochondria of human colon cancer cells (HT-29), acute treatment with the high-affinity TSPO ligand PK11195 promotes a rapid and dose-dependent increase in intracellular Ca^{2+}. This increase is independent of extracellular Ca^{2+} and inhibited by flunitrazepam, a partial TSPO agonist (Ostuni et al., 2007).

In general, mechanisms contributing to regulation of mitochondrial membrane potential and Ca^{2+} homeostasis may involve TSPO interaction with VDAC, which constitutes the principle pathway in the OMM for the transport and exchange of ions, ADP and ATP, as well as metabolites and substrates. VDAC overexpression increases Ca^{2+} permeability at ER-mitochondria contact sites, mitochondrial Ca^{2+} accumulation, and Ca^{2+} transfer between the two organelles (Rapizzi et al., 2002). Moreover, VDAC is co-localized in complex with inositol trisphosphate (IP3) receptors and the glucose-regulated protein 75 (Grp75) at the endoplasmic reticulum (ER)-mitochondria contact sites (Szabadkai et al., 2006), probably promoting Ca^{2+} transfer between the ER and mitochondria (Rodriguez-Arribas et al., 2016). Moreover, Ca^{2+} permeability of VDAC is also regulated by PKA-mediated phosphorylation of VDAC (Gatliff et al., 2017).

3.3. Effect of TSPO ligands on mitochondrial oxidative phosphorylation

Investigating the oxygen consumption rate (OCR) in BV-2 TSPO knockdown cells, we found an increased non-mitochondrial respiration and proton leak, while spare respiratory capacity and coupling efficiency were decreased. Basal respiration, maximal and ATP-related oxygen consumption were unchanged between TSPO knockdown and scramble cells. Experiments which directly targeted TSPO gene expression in specific tissues or in the whole organism revealed inconsistent results. Evidence for TSPO being a modulator of cellular energy metabolism was reported in primary microglia isolated from genetically modified TSPO knock-out mice, where TSPO deficiency was correlated with reduced basal oxygen consumption (Banati et al., 2014). The OCR in mitochondria isolated from a liver-specific conditional TSPO knockout mouse were not different from control mitochondria (Sileikyte et al., 2014). Similarly, steroidogenic mouse MA-10 Leydig cells with eliminated TSPO gene showed no differences in OCR compared to control MA-10 cells (Tu et al., 2014), whereas fibroblasts from global TSPO knock-out mice showed decreased OCR (Zhao et al., 2016). Overexpression of TSPO in Jurkat cells, which show a low level of endogenous TSPO expression, led to the upregulation of proteins involved in electron transport and energy metabolism. This gene regulation correlates with an increased mitochondrial ATP synthesis, cell excitability, motility, and cell proliferation (Liu et al., 2017). These studies demonstrate an impact of TSPO on the modulation of energy metabolism, but also suggest that the effect of TSPO on mitochondrial metabolic parameters, such as OCR, may also be cell-type and tissue dependent.

We found a stimulatory effect of Ro5-4864 and PK11195 on basal and ATP-related respiration, as well as an inhibitory effect on spare respiratory capacity, which was not present in TSPO knock-down cells, arguing for a specific and TSPO-dependent effect on oxygen consumption in BV-2 microglia cells. However, XBD173 promoted a difference in non-mitochondrial respiration only in TSPO knock-down cells. In mouse C1300 neuroblastoma cells, the TSPO ligands PK11195 and Ro5-4864 dose-dependently reduced oxygen consumption (Larcher et al., 1989) and the rate of oxidative phosphorylation in isolated rat kidney mitochondria (Hirsch et al., 1989). Our findings, together with the reports from the literature, indicate that TSPO and TSPO ligands may express differentiated effects on various aspects and levels of energy metabolism, which in part are specific or independent from the expression of TSPO.

3.4. Effect of TSPO ligands on cell proliferation

In line with earlier studies, which reported increased proliferation upon overexpression of TSPO (Xiong et al., 2017), we found a correlation between TSPO expression and cell proliferation in our BV-2 microglia cells. TSPO knockdown cells (untreated) showed a slower proliferation rate compared to scramble cells. However, Bode et al. (2012) reported an increased proliferation of TSPO knockdown U118MG glioblastoma cells (Bode et al., 2012). Moreover, they reported a stimulatory effect of PK11195 (25 μM) on the proliferation of U118MG cells, while this compound (20–60 μM) inhibited proliferation in neuroblastoma cell lines (Mendonca-Torres and Roberts, 2013). In our assay, the proliferation rates of both scramble BV-2 and TSPO knockdown cells were not affected upon treatment with TSPO ligands (10 μM XBD173, 100 nM PK11195, or 100 nM Ro5-4864), although we could show a reduced proliferation after treating scramble BV-2 cells with LPS (100 ng/ml). However, Choi et al. (2011) demonstrated a dose-dependent and interactive effect of LPS, PK11195 and Ro5-4864 on proliferation in primary rat microglia cells (Choi et al., 2011).

In summary, our findings suggest a TSPO-dependent neurosteroid synthesis pathway in microglia cells as well as a direct and TSPO-mediated effect of TSPO ligands on neurosteroid synthesis, MMP, Ca^{2+} homeostasis and energetic metabolism. Moreover, mitochondrial function is differently affected by different TSPO ligands. Off-target effects of TSPO ligands may involve unspecific interaction with lipophilic structures and yet unidentified targets. We suggest that the pharmacological effects of TSPO ligands on specific physiological TSPO-mediated functions most likely depend on the receptor/ligand interaction, and may be affected by TSPO genotype, affinity, and residence time of the ligand, as well as putative conformational changes of the protein, induced or stabilized upon ligand binding. Moreover, TSPO function and effects of TSPO ligands seem to vary in different cell types depending on interacting signaling pathways.

The complexity of the TSPO/TSPO ligand interaction calls for further clarification of the respective underlying mechanisms.

4. Methods

4.1. Cell culture of mouse microglial BV-2 cells

BV-2 mouse microglia cells (gift from M. Karlstetter, University of Cologne, Germany) were grown in Roswell Park Memorial Institute Medium (RPMI 1640 Medium, PAA Laboratories, Cölbe, Germany) supplemented with 10% fetal calf serum (FCS), 2 mM L-glutamine, 10 000U/ml penicillin-streptomycin and 195 nM mercaptoethanol at 37 °C, humidified air and 5% CO_2.

4.2. Lentiviral TSPO knockdown

The Tspo knockdown lentiviral expression vector (pLKO-shTspo) was constructed by replacing the original 1.9 kb stuffer in the pLKO.1 vector using AgeI/EcoRI restriction enzymes by short hairpin double-stranded oligo using the following primers:

mshTSPO-F: 5'-CCGGCCGTGCTCAACTACTATGTATCTCGAGATACATAGTAGTTGAGCACGGTTTTTG-3'

mshTSPO-R: 5'-AATTCAAAAACCGTGCTCAACTACTATGTATCTCGAGATACATAGTAGTTGAGCACGG-3'

pLKO.1-TRC cloning vector was a gift from David Root (Addgene plasmid #10878). The design of the mouse Tspo shRNA was taken from the RNAi Consortium (Moffat et al., 2006) (Cambridge, UK) with the accession number (NM_009775.2). The scramble shRNA was a gift from David Sabatini (Addgene plasmid #1864).

Twenty-four hours before transfection, 2.2×10^6 HEK293 T cells were seeded onto a 100 mm culture dish. Using a standard calcium phosphate transfection protocol, 10 μg of the pLKO.1-shTspo vector, 7.5 μg of psPAX2 (Addgene plasmid #12260), and 2.5 μg of pMD2.G (Addgene plasmid #12259) plasmid were co-transfected into HEK293 T cells. Virus-containing supernatants were collected 48 h after transfection, and were immediately aliquoted and stored at -80C. The titer of lentiviral preparation was determined with colony formation assay using 2 μg/ml puromycin selection and 0.1% Crystal Violet staining solution. Lentiviral transduction was performed by spinoculation at 2400 rpm for 60 min by adding virus solution to cells at the multiplicity of infection of 3–5, which did not show toxic effects on the cells, in the presence of 8 μg/ml polybrene. Fresh BV-2 culture medium containing a 2 μg/ml of puromycin was added to cells 24 h after infection; cells remained under selection until all the mock-transfected cells died. Surviving cells were pooled and cultured for further analysis.

4.3. Immunofluorescence

BV-2 scramble or TSPO knockdown cells were grown for 24 h on sterile glass coverslips and fixed for 10 min at room temperature with 4% (w/v) paraformaldehyde (Carl Roth GmbH, Karlsruhe, Germany). After washing, cells were permeabilized with blocking/permeabilization solution (10% (v/v) goat serum, 0.5% (v/v) Triton X-100 in 1 × PBS) for 20 min. Cells were then incubated overnight, at 4 °C with rabbit-anti-TSPO antibody (ab109497) and mouse-anti-ATPB antibody (ab14730), both from Abcam, Cambridge, UK, diluted 1:1000 in 2% goat serum and 0.1% Triton X-100 in 1 × PBS. After three additional washing steps, cells were incubated for 1 h with secondary antibodies conjugated with Alexa Fluor 488 and Cy3 (Life Technologies, Carlsbad, USA, both diluted 1:1000 in 2% goat serum and 0.1% Triton X-100 in 1 × PBS. Nuclei were labeled with Hoe33342 (AppliChem, Darmstadt, Germany) at a final concentration of 0.1 ug/ml in 1 x PBS. Finally, cells were mounted with confocal matrix (Micro Tech Lab, Graz, Austria) and examined with an inverted fluorescence microscope (Observer.Z1, ZEISS, Jena, Germany). An XBO 175 W served as the light source (Lambda DG4, Sutter instruments, Novato, USA). Images were taken by a ZEISS AxioCam MRm CCD camera using the ZEN software (ZEISS).

4.4. RNA isolation, reverse transcription and quantitative real-time RT-PCR

Total RNA was extracted using RNA Plus Kit (Macherey-Nagel, Düren, Germany) according to the manufacturer´s instructions. First strand cDNA synthesis from 1 μg of total RNA was performed with QuantiTect Reverse Transcription Kit (Qiagen, Hilden, Germany). Quantitative real-time RT-PCR experiments were performed with Rotor-Gene-Q machine (Qiagen, Hilden, Germany) using the 1x Takyon SYBR Master Mix (Eurogentec, Köln, Germany), and specific intron-spanning primers, listed in Supplemental Table 1. Measurements were performed in triplicate and results were analyzed with a Rotor-Gene-Q software version 2.3 (Qiagen, Hilden, Germany) applying the ΔΔCt method for relative quantification.

4.5. Pharmacology

The concentration of compounds in the experiments (10 μM XBD173, 100 nM PK11195, 100 nM Ro5-4864) were adjusted according to the sublethal toxic concentration as demonstrated by the WST-1 viability assay (Sigma-Aldrich) using a range from 1 nM to 100 μM (data not shown). In addition, a lower concentration of XBD173 (1 μM) was tested in some experiments.

The compounds were dissolved in ethanol and diluted with assay buffer to the final working concentration (ethanol concentration below 1:1000). All treatments were compared with solvent control.

4.6. Pregnenolone ELISA

1×10^6 BV-2 scramble or TSPO knockdown cells were grown in RPMI medium at 37 °C, humidified air and 5% CO_2 and incubated with XBD (10 μM), Pk11195 (100 nm), Ro5-4864 (100 nm) or LPS (100 ng/

ml). After 16 h, cells were washed with PBS, and kept in pregnenolone assay buffer (140 mM NaCl, 5 mM KCl, 1.8 mM $CaCl_2$, 1 mM $MgSO_4$, 10 mM glucose and 10 mM HEPES) containing 25 μM trilostane (Sigma Aldrich) to inhibit further metabolism of pregnenolone. Cells were treated again with TSPO ligands or LPS for additional 8 h. Then, supernatants were analyzed using an enzyme-linked immunosorbent assay (ELISA) for pregnenolone quantification, according to the manufacturer's recommendations (Pregnenolone ELISA, IBL International, Hamburg, Germany). Assays were read with a Tecan Spectra microplate reader (Tecan, Crailsheim, Germany) at 450 nm. Data were analyzed by Magellan Data Analysis Software (Tecan, Version 2.0).

4.7. Gas chromatography-mass spectrometry

4.7.1. Sample preparation – derivatisation – GC/nCI-MS analysis

To 1 ml matrix 80 ng internal standard D4-pregnenolone (#Q5500-024, Steraloids, Newport, USA) was added and the mixtures were loaded onto endcapped C18-SPE columns (3 ml/500 mg, Macherey & Nagel, Dueren, Germany). The columns were preconditioned successively with 3 ml methanol and 3 ml of a methanol/water mixture (5/95 V%/V%). The loaded columns were washed with 3 ml methanol/water (5/95 V%/V%), dried under vacuum, and the analytes were eluted with 3 ml methanol. The methanol extracts were dried in a gentle N2-stream at 42 °C and reconstituted in 100 μl ethyl acetate. The target substances in ethyl acetate were derivatized by adding 20 μl heptafluorobutyric acid anhydride (Macherey & Nagel, Dueren, Germany) for 30 min. An additional drying step was accomplished by reconstitution of the residue in 25 μl toluene for GC/nCI-MS analysis. Quantification of pregnenolone, allopregnanolone and tetrahydrodeoxycorticosterone was achieved under the following conditions: GC: HP6890plus, splittless mode at 250 °C injector temperature; MS: HP5973 MSD (both Agilent Technologies, Palo Alto, CA, USA); Column: Optima 5 MS (25m*0.2mm*0.2 μm, Macherey & Nagel, Dueren, Germany); temperature program: 95 °C for 1 min, increase to 210 °C with 30 K/min; hold for 3 min then increase to 235 °C with 2.5 K/min; hold for 9 min then increase to 300 °C with 25 K/min steps; finally hold for 6 min.

Targets and Internal standard (name, retention time, quantifier - and qualifier - ion): Pregnenolone, 27.7 min, 472.4 *m/z*, 492.4 *m/z*; allopregnanolone, 23.9 min, 474.4 *m/z*, 494.4 *m/z*; tetrahydrodeoxycorticosterone, 28.7 min, 512.2 *m/z*, 490.4 *m/z*; D4-pregnenolone, 27.6 min, 476.4 *m/z*, 496.4 *m/z*.

The linearity of calibration was given over the entire range of detected concentrations. The lower limits of quantification (LLOQs) and intraday variabilities (levels: pregnenolone 22 ng/ml; allopregnanolone 3 ng/ml and tetrahydrodeoxycorticosterone 5 ng/ml) were: pregnenolone 1.7 ng/ml, 11%; allopregnanolone 2.9 ng/ml, 22% and tetrahydrodeoxycorticosterone 4.2 ng/ml 19%.

4.8. Mitochondrial membrane potential

2×10^5 BV-2 scramble or TSPO knockdown cells were seeded on sterile glass coverslips (diameter 25 mm), placed in 6 well plates, and grown overnight at 37 °C, humidified air and 5% CO_2. After treating cells for 24 h with XBD (10 μM), Pk11195 (100 nm), Ro5-4864 (100 nm) or LPS (100 ng/ml) in RPMI medium, cells were loaded with 30 nM TMRE/Pluronic (Life Technologies) and 1 μM MitoTracker Green (Life Technologies) in Opti-MEM (Life Technologies) for 30 min at 37 °C, humidified air and 5% CO_2. For imaging, coverslips were washed with assay buffer (140 mM NaCl, 5 mM KCl, 1.8 mM $CaCl_2$, 1 mM $MgSO_4$, 10 mM glucose and 10 mM HEPES) and mounted in a chamber on the inverted microscope (ZEISS Observer Z.1, Jena, Germany). A Lambda DG4 high-speed wavelength switcher (Sutter instruments, Novato, USA) allowed the excitation of TMRE at 545/25 nm and of MitoTracker Green at 470/40 nm. The emitted light was filtered at 605/70 nm and 525/50 nm for red and green fluorescence, respectively, and finally detected by a CCD camera (ZEISS, AxioCam MRm). Mitochondrial membrane potential was analyzed as ratio of TMRE vs. MitoTracker Green fluorescence intensity in regions of interest, drawn over selected cells in the visual field using the Zen imaging software (ZEISS) and ImageJ.

4.9. Ca^{2+} imaging

Ca^{2+} imaging experiments were performed using a ZEISS live cell imaging setup based on a ZEISS Observer Z.1 and images were recorded by using 40x and 20x objective lens as described before (Tang et al., 2013). 30 min before the measurement, cells were loaded with 2 μM Fura-2/AM (Life Technologies) in cell culture medium at 37 °C. The DMSO concentration never exceeded 0.1%. The cell culture medium was replaced by Ringer's solution. Illumination control and image recording were performed using a Lambda DG4 high-speed wavelength switcher (Sutter Instruments) and the Zen imaging software (ZEISS). Ca^{2+} signals were expressed as ratio of the fluorescence intensity during excitation with 340 nm or 380 nm (F340/F380).

4.10. Mitochondrial respirometry

7×10^4 BV-2 scramble or TSPO knockdown cells were grown in XFp 8 well miniplates (Agilent Technologies, Waldbronn, Germany) at 37 °C, humidified air and 5% CO_2, and incubated with XBD (10 μM), Pk11195 (100 nm), Ro5-4864 (100 nm) or LPS (100 ng/ml) for 24 h. Cartridges were prepared according to the manufacture's recommendations. The XFp Cell Mito Stress Test Kit (Agilent Technologies) contained the mitochondrial stress compounds oligomycin (1 μM), FCCP (2 μM), and rotenone/antimycin A (1 μM). Oxygen consumption rate (OCR) and extracellular acidification rate (EACAR) were measured by means of a XFp Seahorse Flux Analyzer (Agilent Technologies).

4.11. Cell growth assay

Cells were plated in 96-well dishes at 500 to 1000 cells per well. Twenty-four h after plating in standard culture media, the solution was replaced with fresh media containing one of the following supplements: 10 μM XBD173, 100 nM PK11195, 100 nM Ro5-4864, or 100 ng/ml LPS. Pictures of the cells were taken using the IncuCyte Live-Cell Imaging System (Essen Bioscience). Experiments were conducted for 150 h and 4 planes of view per well were imaged every 2 h. Live cell images were collected using a 10x objective, and cell confluence was calculated using IncuCyte ZOOM 2016 software, which provides real-time cellular confluence data based on segmentation of phase-contrast images.

4.12. Statistical analysis

Statistical analysis was performed with IBM SPSS Statistics 25 and GraphPad Prism7. Statistical significance was assessed using independent samples t-test, Mann-Whitney U test, or ANOVA, combined with *post hoc* tests for multiple comparisons. Results were regarded statistically significant for $p < 0.05$.

Author contributions

SB, LW, VM and CHW designed the research; SB, LW, VM, MG and CHW performed the experiments; SB, LW, VM, MG, CN, RR and CHW analyzed the data; CHW wrote the paper.

Competing interests

The authors declare that they have no competing interests.

Acknowledgement

This work has been supported by the German Research Foundation DFG (WE2298). We are grateful to Prof. Dr. Philipp Beckhove and Dr. Till Michels (Regensburg Center for Interventional Immunology) for their help with the cell proliferation assay. The authors would also like to thank T. Jahner, H. Hallof-Büstrich and D. Melchner for their technical assistance, and to Mr. Evan H. Stanton for his constructive criticism of the manuscript.

Appendix A. Supplementary data

Supplementary material related to this article can be found, in the online version, at doi:https://doi.org/10.1016/j.psyneuen.2019.03.029.

References

Banati, R.B., Middleton, R.J., Chan, R., Hatty, C.R., Kam, W.W., Quin, C., Graeber, M.B., Parmar, A., Zahra, D., Callaghan, P., Fok, S., Howell, N.R., Gregoire, M., Szabo, A., Pham, T., Davis, E., Liu, G.J., 2014. Positron emission tomography and functional characterization of a complete PBR/TSPO knockout. Nat. Commun. 5, 5452.

Bode, J., Veenman, L., Caballero, B., Lakomek, M., Kugler, W., Gavish, M., 2012. The 18 kDa translocator protein influences angiogenesis, as well as aggressiveness, adhesion, migration, and proliferation of glioblastoma cells. Pharmacogenet. Genomics 22, 538–550.

Chaudhuri, D., Artiga, D.J., Abiria, S.A., Clapham, D.E., 2016. Mitochondrial calcium uniporter regulator 1 (MCUR1) regulates the calcium threshold for the mitochondrial permeability transition. Proc. Natl. Acad. Sci. U. S. A. 113, E1872–1880.

Chen, Z.H., Jalabi, W., Shpargel, K.B., Farabaugh, K.T., Dutta, R., Yin, X.H., Kidd, G.J., Bergmann, C.C., Stohlman, S.A., Trapp, B.D., 2012. Lipopolysaccharide-induced microglial activation and neuroprotection against experimental brain injury is independent of hematogenous TLR4. J. Neurosci. 32, 11706–11715.

Choi, J., Ifuku, M., Noda, M., Guilarte, T.R., 2011. Translocator protein (18 kDa)/peripheral benzodiazepine receptor specific ligands induce microglia functions consistent with an activated state. Glia 59, 219–230.

Cosenza-Nashat, M., Zhao, M.L., Suh, H.S., Morgan, J., Natividad, R., Morgello, S., Lee, S.C., 2009. Expression of the translocator protein of 18 kDa by microglia, macrophages and astrocytes based on immunohistochemical localization in abnormal human brain. Neuropathol. Appl. Neurobiol. 35, 306–328.

Costa, B., Da Pozzo, E., Cavallini, C., Taliani, S., Da Settimo, F., Martini, C., 2016a. Long residence time at the neurosteroidogenic 18 kDa translocator protein characterizes the anxiolytic ligand XBD173. ACS Chem. Neurosci. 7, 1041–1046.

Costa, B., Da Pozzo, E., Giacomelli, C., Barresi, E., Taliani, S., Da Settimo, F., Martini, C., 2016b. TSPO ligand residence time: a new parameter to predict compound neurosteroidogenic efficacy. Sci. Rep. 6, 18164.

Costa, B., Da Pozzo, E., Martini, C., 2018. Translocator protein and steroidogenesis. Biochem. J. 475, 901–904.

Da Pozzo, E., Giacomelli, C., Costa, B., Cavallini, C., Taliani, S., Barresi, E., Da Settimo, F., Martini, C., 2016. TSPO PIGA ligands promote neurosteroidogenesis and human astrocyte well-being. Int. J. Mol. Sci. 17.

Do-Rego, J.L., Mensah-Nyagan, A.G., Feuilloley, M., Ferrara, P., Pelletier, G., Vaudry, H., 1998. The endozepine triakontatetraneuropeptide diazepam-binding inhibitor [17–50] stimulates neurosteroid biosynthesis in the frog hypothalamus. Neuroscience 83, 555–570.

File, S.E., Lister, R.G., 1983. The anxiogenic action of Ro 5-4864 is reversed by phenytoin. Neurosci. Lett. 35, 93–96.

Gatliff, J., East, D., Crosby, J., Abeti, R., Harvey, R., Craigen, W., Parker, P., Campanella, M., 2014. TSPO interacts with VDAC1 and triggers a ROS-mediated inhibition of mitochondrial quality control. Autophagy 10, 2279–2296.

Gatliff, J., East, D.A., Singh, A., Alvarez, M.S., Frison, M., Matic, I., Ferraina, C., Sampson, N., Turkheimer, F., Campanella, M., 2017. A role for TSPO in mitochondrial Ca2+ homeostasis and redox stress signaling. Cell Death Dis. 8, e2896.

Gilbert, D.F., Stebbing, M.J., Kuenzel, K., Murphy, R.M., Zacharewicz, E., Buttgereit, A., Stokes, L., Adams, D.J., Friedrich, O., 2016. Store-operated Ca(2+) entry (SOCE) and purinergic receptor-mediated Ca(2+) homeostasis in murine bv2 microglia cells: early cellular responses to ATP-Mediated microglia activation. Front. Mol. Neurosci. 9, 111.

Giorgi, C., Baldassari, F., Bononi, A., Bonora, M., De Marchi, E., Marchi, S., Missiroli, S., Patergnani, S., Rimessi, A., Suski, J.M., Wieckowski, M.R., Pinton, P., 2012. Mitochondrial Ca2+ and apoptosis. Cell Calcium 52, 36–43.

Hirsch, J.D., Beyer, C.F., Malkowitz, L., Beer, B., Blume, A.J., 1989. Mitochondrial benzodiazepine receptors mediate inhibition of mitochondrial respiratory control. Mol. Pharmacol. 35, 157–163.

Kim, T., Pae, A.N., 2016a. Translocator protein (TSPO) ligands for the diagnosis or treatment of neurodegenerative diseases: a patent review (2010-2015; part 1). Expert Opin. Ther. Pat. 26, 1325–1351.

Kim, T., Pae, A.N., 2016b. Translocator protein (TSPO) ligands for the diagnosis or treatment of neurodegenerative diseases: a patent review (2010–2015; part 2). Expert Opin. Ther. Pat. 26, 1353–1366.

Korneyev, A., Pan, B.S., Polo, A., Romeo, E., Guidotti, A., Costa, E., 1993. Stimulation of brain pregnenolone synthesis by mitochondrial diazepam binding inhibitor receptor ligands in vivo. J. Neurochem. 61, 1515–1524.

Kozikowski, A.P., Ma, D., Brewer, J., Sun, S., Costa, E., Romeo, E., Guidotti, A., 1993. Chemistry, binding affinities, and behavioral properties of a new class of "anti-neophobic" mitochondrial DBI receptor complex (mDRC) ligands. J. Med. Chem. 36, 2908–2920.

Larcher, J.C., Vayssiere, J.L., Le Marquer, F.J., Cordeau, L.R., Keane, P.E., Bachy, A., Gros, F., Croizat, B.P., 1989. Effects of peripheral benzodiazepines upon the O2 consumption of neuroblastoma cells. Eur. J. Pharmacol. 161, 197–202.

Le Fur, G., Perrier, M.L., Vaucher, N., Imbault, F., Flamier, A., Benavides, J., Uzan, A., Renault, C., Dubroeucq, M.C., Gueremy, C., 1983. Peripheral benzodiazepine binding sites: effect of PK 11195, 1-(2-chlorophenyl)-N-methyl-N-(1-methylpropyl)-3-isoquinolinecarboxamide. I. In vitro studies. Life Sci. 32, 1839–1847.

Liu, G.J., Middleton, R.J., Kam, W.W., Chin, D.Y., Hatty, C.R., Chan, R.H., Banati, R.B., 2017. Functional gains in energy and cell metabolism after TSPO gene insertion. Cell Cycle 16, 436–447.

McEnery, M.W., Snowman, A.M., Trifiletti, R.R., Snyder, S.H., 1992. Isolation of the mitochondrial benzodiazepine receptor: association with the voltage-dependent anion channel and the adenine nucleotide carrier. Proc. Natl. Acad. Sci. U. S. A. 89, 3170–3174.

Mendonca-Torres, M.C., Roberts, S.S., 2013. The translocator protein (TSPO) ligand PK11195 induces apoptosis and cell cycle arrest and sensitizes to chemotherapy treatment in pre- and post-relapse neuroblastoma cell lines. Cancer Biol. Ther. 14, 319–326.

Moffat, J., Grueneberg, D.A., Yang, X., Kim, S.Y., Kloepfer, A.M., Hinkle, G., Piqani, B., Eisenhaure, T.M., Luo, B., Grenier, J.K., Carpenter, A.E., Foo, S.Y., Stewart, S.A., Stockwell, B.R., Hacohen, N., Hahn, W.C., Lander, E.S., Sabatini, D.M., Root, D.E., 2006. A lentiviral RNAi library for human and mouse genes applied to an arrayed viral high-content screen. Cell 124, 1283–1298.

Morohaku, K., Pelton, S.H., Daugherty, D.J., Butler, W.R., Deng, W., Selvaraj, V., 2014. Translocator protein/peripheral benzodiazepine receptor is not required for steroid hormone biosynthesis. Endocrinology 155, 89–97.

Ostuni, M.A., Ducroc, R., Peranzi, G., Tonon, M.C., Papadopoulos, V., Lacapere, J.J., 2007. Translocator protein (18 kDa) ligand PK 11195 induces transient mitochondrial Ca2+ release leading to transepithelial Cl- secretion in HT-29 human colon cancer cells. Biol. Cell 99, 639–647.

Owen, D.R., Fan, J., Campioli, E., Venugopal, S., Midzak, A., Daly, E., Harlay, A., Issop, L., Libri, V., Kalogiannopoulou, D., Oliver, E., Gallego-Colon, E., Colasanti, A., Huson, L., Rabiner, I., Suppiah, P., Essagian, C., Matthews, P.M., Papadopoulos, V., 2017. TSPO mutations in rats and a human polymorphism impair the rate of steroid synthesis. Biochem. J. 474, 3985–3999.

Palzur, E., Sharon, A., Shehadeh, M., Soustiel, J.F., 2016. Investigation of the mechanisms of neuroprotection mediated by Ro5-4864 in brain injury. Neuroscience 329, 162–170.

Papadopoulos, V., Lecanu, L., 2009. Translocator protein (18 kDa) TSPO: an emerging therapeutic target in neurotrauma. Exp. Neurol. 219, 53–57.

Papadopoulos, V., Baraldi, M., Guilarte, T.R., Knudsen, T.B., Lacapere, J.J., Lindemann, P., Norenberg, M.D., Nutt, D., Weizman, A., Zhang, M.R., Gavish, M., 2006. Translocator protein (18kDa): new nomenclature for the peripheral-type benzodiazepine receptor based on its structure and molecular function. Trends Pharmacol. Sci. 27, 402–409.

Papadopoulos, V., Aghazadeh, Y., Fan, J., Campioli, E., Zirkin, B., Midzak, A., 2015. Translocator protein-mediated pharmacology of cholesterol transport and steroidogenesis. Mol. Cell. Endocrinol. 408, 90–98.

Papadopoulos, V., Fan, J., Zirkin, B., 2017. Translocator protein (18 kDa): an update on its function in steroidogenesis. J. Neuroendocrinol. 30. https://doi.org/10.1111/jne.12500.

Rapizzi, E., Pinton, P., Szabadkai, G., Wieckowski, M.R., Vandecasteele, G., Baird, G., Tuft, R.A., Fogarty, K.E., Rizzuto, R., 2002. Recombinant expression of the voltage-dependent anion channel enhances the transfer of Ca2+ microdomains to mitochondria. J. Cell Biol. 159, 613–624.

Rodriguez-Arribas, M., Yakhine-Diop, S.M., Pedro, J.M., Gomez-Suaga, P., Gomez-Sanchez, R., Martinez-Chacon, G., Fuentes, J.M., Gonzalez-Polo, R.A., Niso-Santano, M., 2016. Mitochondria-associated membranes (MAMs): overview and its role in parkinson's disease. Mol. Neurobiol. 54, 6287–6303.

Rupprecht, R., Papadopoulos, V., Rammes, G., Baghai, T.C., Fan, J., Akula, N., Groyer, G., Adams, D., Schumacher, M., 2010. Translocator protein (18 kDa) (TSPO) as a therapeutic target for neurological and psychiatric disorders. Nat. Rev. Drug Discov. 9, 971–988.

Selvaraj, V., Tu, L.N., 2016. Current status and future perspectives: TSPO in steroid neuroendocrinology. J. Endocrinol. 231, R1–R30.

Sileikyte, J., Blachly-Dyson, E., Sewell, R., Carpi, A., Menabo, R., Di Lisa, F., Ricchelli, F., Bernardi, P., Forte, M., 2014. Regulation of the mitochondrial permeability transition pore by the outer membrane does not involve the peripheral benzodiazepine receptor (Translocator Protein of 18 kDa (TSPO)). J. Biol. Chem. 289, 13769–13781.

Szabadkai, G., Bianchi, K., Varnai, P., De Stefani, D., Wieckowski, M.R., Cavagna, D., Nagy, A.I., Balla, T., Rizzuto, R., 2006. Chaperone-mediated coupling of endoplasmic reticulum and mitochondrial Ca2+ channels. J. Cell Biol. 175, 901–911.

Tang, Z., Kim, A., Masuch, T., Park, K., Weng, H., Wetzel, C., Dong, X., 2013. Pirt functions as an endogenous regulator of TRPM8. Nat. Commun. 4, 2179.

Tu, L.N., Morohaku, K., Manna, P.R., Pelton, S.H., Butler, W.R., Stocco, D.M., Selvaraj, V., 2014. Peripheral benzodiazepine receptor/translocator protein global knock-out mice are viable with no effects on steroid hormone biosynthesis. J. Biol. Chem. 289, 27444–27454.

Tu, L.N., Zhao, A.H., Stocco, D.M., Selvaraj, V., 2015. PK11195 effect on steroidogenesis

is not mediated through the translocator protein (TSPO). Endocrinology 156, 1033–1039.
Tu, L.N., Zhao, A.H., Hussein, M., Stocco, D.M., Selvaraj, V., 2016. Translocator protein (TSPO) affects mitochondrial fatty acid oxidation in steroidogenic cells. Endocrinology 157, 1110–1121.
Vasington, F.D., Murphy, J.V., 1962. Ca ion uptake by rat kidney mitochondria and its dependence on respiration and phosphorylation. J. Biol. Chem. 237, 2670–2677.
Weissman, B.A., Cott, J., Hommer, D., Quirion, R., Paul, S., Skolnick, P., 1983. Pharmacological, electrophysiological, and neurochemical actions of the convulsant benzodiazepine Ro 5-4864 (4'-chlordiazepam). Adv. Biochem. Psychopharmacol. 38, 139–151.
Wolf, L., Bauer, A., Melchner, D., Hallof-Buestrich, H., Stoertebecker, P., Haen, E., Kreutz, M., Sarubin, N., Milenkovic, V.M., Wetzel, C.H., Rupprecht, R., Nothdurfter, C., 2015. Enhancing neurosteroid synthesis–relationship to the pharmacology of translocator protein (18 kDa) (TSPO) ligands and benzodiazepines. Pharmacopsychiatry 48, 72–77.
Xiong, S., Wang, B., Lin, S., Zhang, H., Li, Y., Wei, X., Cui, Y., Wei, X., Lu, Z., Gao, P., Li, L., Zhao, Z., Liu, D., Zhu, Z., 2017. Activation of transient receptor potential melastatin subtype 8 attenuates cold-induced hypertension through ameliorating vascular mitochondrial dysfunction. J. Am. Heart Assoc. 6.
Zhang, L.M., Zhao, N., Guo, W.Z., Jin, Z.L., Qiu, Z.K., Chen, H.X., Xue, R., Zhang, Y.Z., Yang, R.F., Li, Y.F., 2014. Antidepressant-like and anxiolytic-like effects of YL-IPA08, a potent ligand for the translocator protein (18 kDa). Neuropharmacology 81, 116–125.
Zhao, A.H., Tu, L.N., Mukai, C., Sirivelu, M.P., Pillai, V.V., Morohaku, K., Cohen, R., Selvaraj, V., 2016. Mitochondrial translocator protein (TSPO) function is not essential for heme biosynthesis. J. Biol. Chem. 291, 1591–1603.